PHYSICS

Deterministic quantum teleportation through fiber channels

Meiru Huo[1], Jiliang Qin[1], Jialin Cheng[1], Zhihui Yan[1,2], Zhongzhong Qin[1,2], Xiaolong Su[1,2], Xiaojun Jia[1,2]*, Changde Xie[1,2], Kunchi Peng[1,2]

Quantum teleportation, which is the transfer of an unknown quantum state from one station to another over a certain distance with the help of nonlocal entanglement shared by a sender and a receiver, has been widely used as a fundamental element in quantum communication and quantum computation. Optical fibers are crucial information channels, but teleportation of continuous variable optical modes through fibers has not been realized so far. Here, we experimentally demonstrate deterministic quantum teleportation of an optical coherent state through fiber channels. Two sub-modes of an Einstein-Podolsky-Rosen entangled state are distributed to a sender and a receiver through a 3.0-km fiber, which acts as a quantum resource. The deterministic teleportation of optical modes over a fiber channel of 6.0 km is realized. A fidelity of 0.62 ± 0.03 is achieved for the retrieved quantum state, which breaks through the classical limit of $^1/_2$. Our work provides a feasible scheme to implement deterministic quantum teleportation in communication networks.

INTRODUCTION

Quantum teleportation is a reliable protocol for transferring quantum states under the help of entanglement. At first, two subsystems of a prepared entangled state are distributed to a sender and a distant receiver. Then, an input quantum state is jointly measured together with one-half of the entangled state hold by the sender. Successively, the measurement results are transmitted to the receiver through classical channels. Last, the other half of the entangled state hold by the receiver is transformed via a basic operation with the received measurement results to retrieve the teleported state. During the teleporting process, the quantum state is not transferred directly; only its quantum and classical information are sent to the receiver by means of quantum entanglement and classical channels, respectively. The input quantum state is destroyed by the joint measurement at the sending station and retrieved at the receiving station; thus, the purification of the input state will not be influenced by the loss and extra noise in the transmission channels (1). Since Bennett et al. proposed quantum teleportation in 1993, various researches on theoretical analysis and experimental implementation have been successively completed (1–6). Quantum teleportation serves as the cornerstone for building quantum information networks, and it also greatly contributes to completing quantum computation and quantum communication (7–9). A variety of quantum information protocols, such as entanglement swapping, quantum repeaters, quantum teleportation networks, quantum gate teleportation, and quantum computation, have already been realized by applying quantum teleportation (10–17). Because of the relatively simple generation system and negligible decoherence from noise environment, single-photon qubits have become important physical carriers to realize quantum teleportation over long distances (18–23). In 2003, Gisin and colleagues accomplished quantum teleportation of qubits with a 2.0-km standard telecommunication fiber, in which the transmission distance of a quantum state on the order of kilometers was first reached in the discrete variable region (18). Then, quantum teleportation over 100 km was implemented by Pan's and Zeilinger's groups separately (19, 20). Very recently, by means of a low–Earth orbit satellite, ground-to-satellite

quantum teleportation with a single photon over 1400 km was achieved, which provided a feasible protocol to realize quantum communication at a global scale (23). Although great progress has been made for demonstrating quantum teleportation of photonic qubits, a probabilistic generation method forms an obstacle to develop instantaneous transfer of quantum states without post-selection. Thus, it is necessary to explore near-deterministic quantum teleportation protocols in quantum communication and teleportation-based quantum computation (9). Continuous variable (CV) quantum teleportation of optical modes, which is based on entangled states of light, can realize unconditional and deterministic transfer of arbitrary unknown quantum states (3, 4). Transfer and retrieval for both coherent and nonclassical states, such as squeezed state, entangled state, photonic quantum bits, and Schrödinger's cat state, have been experimentally realized with CV quantum teleportation method in free space (10, 24–27). Nevertheless, all these quantum teleportation experiments in the CV region are implemented in laboratories, and the transmission distance is very short. For practical applications of CV quantum teleportation, a key challenge is to extend possible transfer distance.

Here, we report the first experimental realization of CV quantum teleportation through optical fiber channels. Two sub-modes of a CV entangled state of light are distributed to the sender (Alice) and the receiver (Bob) through a 3.0-km-long optical fiber which means that the total fiber length between Alice and Bob is 6.0 km. The fidelity of the retrieved coherent state is about 0.62 ± 0.03, which is higher than the classical limit of $^1/_2$. Furthermore, a fidelity of 0.69 ± 0.03 breaking through the no-cloning limit of $^2/_3$ (28, 29) has also been achieved when the transmission distance is 2.0 km.

RESULTS

Schematic of CV fiber-channel quantum teleportation

The schematic for CV quantum teleportation through fiber channels is shown in Fig. 1, which includes a resource station for providing an Einstein-Podolsky-Rosen (EPR) entangled state of light, a sending station (Alice), and a receiving station (Bob). These stations are connected by optical fibers that are used as quantum channels. In quantum optics theory, a coherent state is defined as the eigenstate of an annihilation operator, and its dynamics most closely resembles that of a classical harmonic oscillator. The expectation values of amplitude and phase

[1]State Key Laboratory of Quantum Optics and Quantum Optics Devices, Institute of Opto-Electronics, Shanxi University, Taiyuan 030006, China. [2]Collaborative Innovation Center of Extreme Optics, Shanxi University, Taiyuan 030006, China.
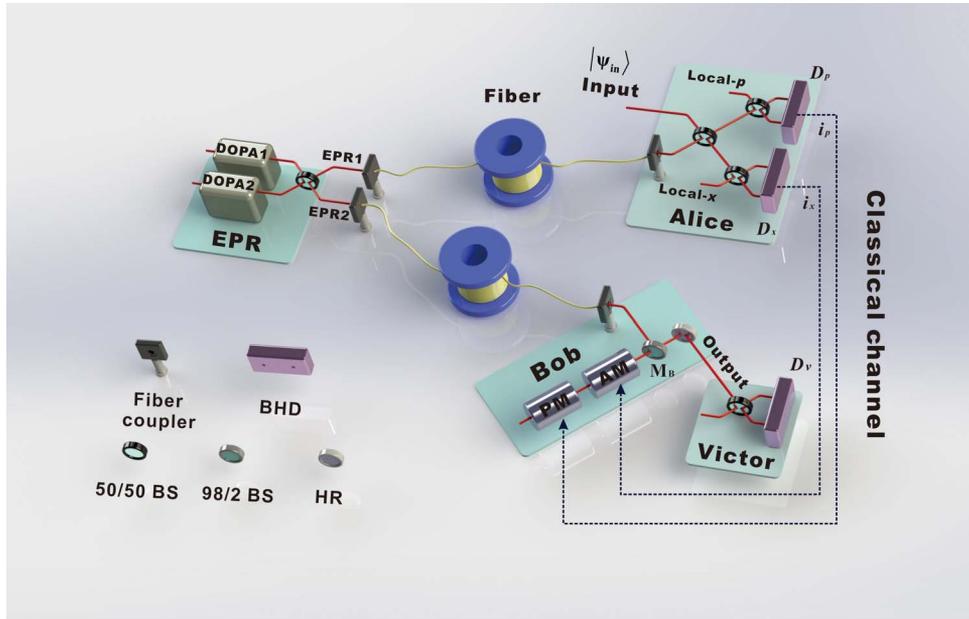*Corresponding author. Email: jiaxj@sxu.edu.cn

Fig. 1. Experimental scheme of fiber-channel CV quantum teleportation. Two single-mode squeezed states generated by a pair of degenerate optical parametric amplifiers (DOPAs) are coupled to produce an EPR entangled state. The two sub-modes of the EPR entangled state are sent to Alice and Bob through two optical fiber channels, respectively. Then, Alice implements a joint measurement on the unknown input state and the sub-mode EPR1 and sends the measured results to Bob through classical channels. Bob implements a translation for EPR2 by coupling a coherent beam, which is modulated by two joint-measured classical signals, respectively, via an AM and a PM. Last, Victor accomplishes the verification for quantum teleportation. 98/2 BS, beam splitter with reflectivity of 98%; HR, mirror with a reflectivity larger than 99.9%; fiber coupler, used to couple optical modes into the fiber; BHD, balance homodyne detector.

quadrature operators of a coherent state are equal to their classical values. The coherent state is a minimum uncertainty state, and its uncertainty is split equally between two quadrature components. It is the closest quantum approximation of an optical field generated by a laser; thus, the coherent state is usually selected as the input state in CV quantum optical experiments (4). In the experiment, EPR entanglement is obtained by coupling two single-mode squeezed states of light, which are generated from a pair of DOPAs operating below their oscillation threshold, at a 50/50 beam splitter (50/50 BS). The wavelength of EPR entangled optical modes is chosen at 1.34 μm (30), which is close to the transmission window of the commercial fiber at 1.3 μm. The amplitude quadrature ($\hat{x}$) and the phase quadrature ($\hat{p}$) of two sub-modes of an EPR entangled state (EPR1 and EPR2) are expressed by $\hat{x}_{\text{EPR1(2)}} = \hat{a}_{\text{EPR1(2)}} + \hat{a}^+_{\text{EPR1(2)}}$ and $\hat{p}_{\text{EPR1(2)}} = (\hat{a}_{\text{EPR1(2)}} - \hat{a}^+_{\text{EPR1(2)}})/i$, respectively, where $\hat{a}$ and $\hat{a}^+$ are annihilation and creation operators of the electromagnetic field, respectively. There are strong quantum correlations between quadrature components of two EPR sub-modes; i.e., the correlation variances of both quadrature amplitude sum $\langle\delta^2(\hat{x}_{\text{EPR1}} + \hat{x}_{\text{EPR2}})\rangle = 2e^{-2r}$ and quadrature phase difference $\langle\delta^2(\hat{p}_{\text{EPR1}} - \hat{p}_{\text{EPR2}})\rangle = 2e^{-2r}$ are lower than the corresponding quantum noise limits (QNLs), where r ($0 \leq r < \infty$) is the correlation factor (30). Meanwhile, the anti-squeezing quantum noise levels of amplitude difference $\langle\delta^2(\hat{x}_{\text{EPR1}} - \hat{x}_{\text{EPR2}})\rangle = 2e^{2r}$ and phase sum $\langle\delta^2(\hat{p}_{\text{EPR1}} + \hat{p}_{\text{EPR2}})\rangle = 2e^{2r}$ are much higher than the corresponding QNLs (8). During quantum teleportation, two sub-modes of the EPR entangled state are first sent to Alice and Bob through an optical fiber. Then, the sub-mode received by Alice ($\hat{a}_{\text{EPR1}}$) and the unknown quantum state (input state, $|\psi_{\text{in}}\rangle = |\hat{x}_{\text{in}} + i\hat{p}_{\text{in}}\rangle$) are combined on a 50/50 BS. The amplitude quadrature $\hat{x}_{\text{tel}} = (\hat{x}_{\text{in}} + \hat{x}_{\text{EPR1}})/\sqrt{2}$ and the phase quadrature $\hat{p}_{\text{tel}} = (\hat{p}_{\text{in}} - \hat{p}_{\text{EPR1}})/\sqrt{2}$ of two output fields of the 50/50 BS are measured by two sets of balanced homodyne detectors (D_x and D_p) with local oscillators (LOs) (local x

and local p), respectively. These joint measurements of the input state and the sub-mode EPR1 provide an analogy of Bell-state measurement in the CV region (5, 31, 32). If a perfect EPR entangled state ($r \rightarrow \infty$) is used, then Alice will not be able to obtain any information about the input state. The results measured by Alice (i_x, i_p) are transmitted to Bob via two classical channels. Bob modulates his own sub-mode of the EPR entangled state ($\hat{a}_{\text{EPR2}}$) with the received measurement results, which is realized by means of an amplitude electro-optic modulator (AM) and a phase electro-optic modulator (PM). In this way, the input quantum state destroyed by the joint measurements at Alice is recovered by Bob under the help of nonlocal quantum entanglement (3). Last, Victor performs the verification measurements of teleportation results with a homodyne detector (D_V).

Fidelity of recovered quantum state

In quantum teleportation experiments, the output state of Bob is sent to Victor to verify whether quantum teleportation has been successfully implemented. Fidelity F is usually used to quantify the performance of quantum teleportation (29)

$$F = \langle\psi_{\text{in}}|\rho_{\text{out}}|\psi_{\text{in}}\rangle \tag{1}$$

which represents the overlap between the input state $|\psi_{\text{in}}\rangle$ and the output state characterized by the density matrix ρ_{out}. If detectors with perfect unitary efficiencies are used in the experiment, then the fidelity of quantum teleportation for a coherent input state is expressed by (31)

$$F = \frac{2}{\sigma_Q}\exp\left[-\frac{2}{\sigma_Q}|\beta_{\text{out}} - \beta_{\text{in}}|^2\right] \tag{2}$$

where

$$\sigma_Q = \sqrt{(1 + \sigma_W{}^x)(1 + \sigma_W{}^p)}$$

$$\sigma_W^x = \sigma_W^p = g^2 + \frac{1}{2}e^{2r}(1-g)^2 + \frac{1}{2}e^{-2r}(1+g)^2 \quad (3)$$

σ_Q is the variance of the teleported state in representation of the Q function, which depends on fluctuation variances of amplitude and phase quadratures (σ_W^x and σ_W^p). β_{in} and β_{out} are amplitudes of the input state at Alice and the output state at Bob, respectively. g is the gain factor of the classical channels, which usually has an equivalent value for amplitude (g_x) and phase (g_p) quadratures. In the fiber-channel quantum teleportation system, the influence of transmission efficiency and extra noise inside fibers cannot be neglected because of their observable effect on quantum features of the entanglement. Thus, the coupling efficiency of the fiber coupler (η_C) and the transmission efficiency in fiber (η_F) have to be involved in the calculation of fidelity. The extra noises resulting from fiber channels will reduce entanglement and thus decrease the distance of quantum teleportation. In general, the potential sources of noise in fibers include guided acoustic wave Brillouin scattering (GAWBS), Rayleigh scattering, Raman scattering, and so on. Because of its scattering level and impact frequency range, the extra noise generated by the GAWBS forms a notable thermal noise in fiber channels, the effect of which on quantum entanglement distribution and quantum communication is notable and thus has to be considered (33, 34). In our experiment, a sub-mode of the EPR entangled state and the LO beam are simultaneously transferred in an optical fiber of length l with polarization multiplexing to conveniently lock their relative phase. The depolarized GAWBS scatters some horizontal polarization photons of the LO beam into the signal beam with vertical polarization, which constitutes a thermal-noise source: $\sigma_G^x = \sigma_G^p = \xi l \bar{n}_L$, where ξ is the scattering efficiency per kilometer of fiber and $\bar{n}_L$ is the average photon number of the corresponding LO beam (34). The imperfect detection efficiencies (η_V^2, η_A^2) and finite EPR entanglement have to be considered as well. Hence, the variances (σ_V^x and σ_V^p) measured by the verifier Victor are expressed by

$$\sigma_V^x = 1 - r_B^2\eta_V^2 - g_x^2 + \frac{2g_x^2}{\eta_A^2} + \frac{\sigma^-}{2} \times (g_x + r_B\eta_V)^2 + \frac{\sigma^+}{2} \times (g_x - r_B\eta_V)^2$$

$$\sigma_V^p = 1 - r_B^2\eta_V^2 - g_p^2 + \frac{2g_p^2}{\eta_A^2} + \frac{\sigma^-}{2} \times (g_p + r_B\eta_V)^2 + \frac{\sigma^+}{2} \times (g_p - r_B\eta_V)^2$$

$$(4)$$

where

$$\sigma^- = (1 - \xi l)\eta_C\eta_F e^{-2r} + \eta_C\eta_F\xi^2 l^2 \bar{n}_L + (2 - \eta_C - \eta_F + \xi l)$$

$$\sigma^+ = (1 - \xi l)\eta_C\eta_F e^{2r} + \eta_C\eta_F\xi^2 l^2 \bar{n}_L + (2 - \eta_C - \eta_F + \xi l) \quad (5)$$

$r_B^2 = 0.98$ is the reflectivity of the coupling mirror (M_B) in Bob's station. g_x (g_p) is the gain factor of the classical channel for the amplitude (phase) quadrature component of the input state. In our experiment, the teleportation gains of amplitude quadrature and phase quadrature always take the same values ($g_x = g_p = g$) because the two quadrature components are symmetric. The transmission efficiency of EPR sub-modes in the optical fiber consists of the coupling efficiency $\eta_C = 0.9$ of the fiber

coupler and the transmission efficiency $\eta_F = 10^{-\frac{0.35 \times l}{10}}$ inside the fiber. $\eta_A^2 = 0.95$ and $\eta_V^2 = 0.95$ are quantum efficiencies of the photoelectric detectors in Alice's and Victor's stations, respectively.

With the increasing power of the LO beam, the induced GAWBS extra noise is enhanced, and thus, the quantum entanglement between the sender (Alice) and the receiver (Bob) is decreased. Obviously, the transmission distance is notably influenced by the GAWBS extra noise. The dependences of fidelities of quantum teleportation on the communication distance between Alice and Bob for different powers of LO beams are shown in Fig. 2, where the actual physical parameters of our experimental system are applied in the calculation. The blue, red, yellow, and green curves express the calculated dependences of fidelities on the communication distance between Alice and Bob when the powers of LO beams are 0.25, 0.50, 1.00, and 2.50 mW, respectively. If the fidelity of quantum teleportation decreases below the classical limit of $^1/_2$, then the quantum teleportation is unsuccessful. The squares mark the experimental results, which are in reasonable agreement with the theoretical values.

Experimental system and results

The detailed experimental schematic is introduced in Materials and Methods. DOPA1 and DOPA2, which are constructed in the same configuration, produce two squeezed states of light with the same spatial pattern and an identical optical frequency. The pump power of DOPA1 (DOPA2) is 15 mW (16 mW), which is below its threshold pump power of 23 mW (24 mW). The relative phase between the pump beam and the injected signal beam for each DOPA is locked at $\pi + 2k\pi$ (k is an integer) to enforce the DOPA operating under deamplification conditions (30).
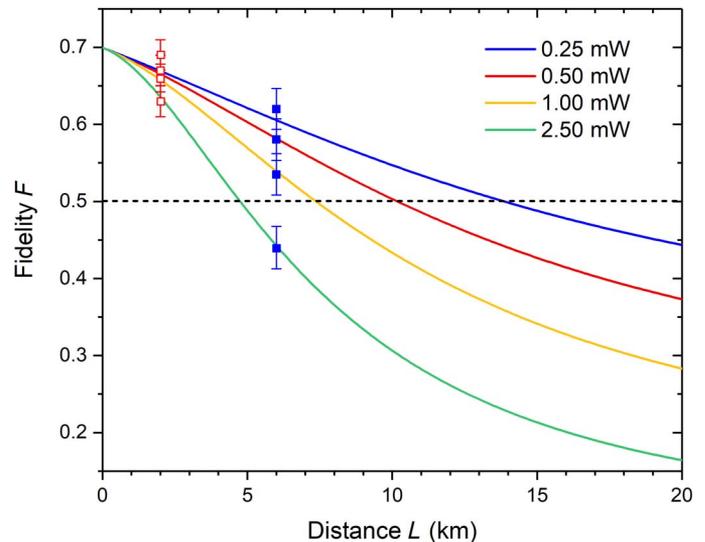

Fig. 2. Fidelity of quantum teleportation versus the communication distance between Alice and Bob for different powers of the LO beam. The blue, red, yellow, and green curves express the calculated dependences of fidelities on the communication distance between Alice and Bob when the power of the LO beam is 0.25, 0.50, 1.00, and 2.50 mW, respectively. With the increasing power of the LO beam, the induced GAWBS extra noise gradually reduces the quantum entanglement between the sender (Alice) and the receiver (Bob). If the fidelity of quantum teleportation decreases below the classical limit of $^1/_2$, then the process is unsuccessful. It can be seen that the fidelity drops quickly when the power of the LO beam is increased because the LO beam with higher power induces more GAWBS noise in the fiber channels. The squares mark the experimental results, which are in reasonable agreement with the theoretical values. Error bars represent the SE and are obtained from the statistics of the fidelity.

Under deamplification conditions, the quadrature amplitude squeezed state of light with 5.28 ± 0.16 dB (5.31 ± 0.19 dB) below the corresponding QNL is generated by DOPA1 (DOPA2). Although higher squeezing is possibly obtained with a larger pump power in principle, the extra noise in the anti-squeezing quadrature component also increases (35). Then, the two squeezed states are coupled to produce an EPR entangled state by a 50/50 BS, and the relative phase between these two squeezed states is maintained at $\pi/2 + k\pi$ (k is an integer). The measured correlation variances of both quadrature amplitude sum and quadrature phase difference are 5.21 ± 0.18 dB and 5.18 ± 0.20 dB below the corresponding QNL, respectively. To realize long-distance CV quantum teleportation, the sub-mode EPR1 (EPR2) with the corresponding LO beam (0.25 mW) is sent to Alice (Bob) through a fiber with polarization multiplexing. In Alice's station, an unknown input state and EPR1 are performed a joint measurement using two sets of homodyne detectors to measure amplitude and phase quadratures, respectively. The resulting signals are sent to Bob through classical channels to retrieve the input state with EPR2. To implement the transformation, the amplitude and phase quadratures of a coherent beam in Bob's station are modulated by the received classical amplitude and phase information using an AM and a PM, respectively. The modulated beam is coupled with EPR2 at the mirror M_B with a reflectivity of 0.98. The obtained output state of M_B closely mimics the original unknown state, and thus, the teleportation of a coherent state of light is completed. Last, the third partner (Victor) measures noise powers and Wigner functions of resultant states and calculates fidelities to verify whether the quantum teleportation is successful or not.

The noise powers of the teleported state at an analysis frequency of 3.0 MHz measured by Victor's balanced homodyne detector are shown in Fig. 3 (A and B), where two sub-modes of the EPR entangled state are separately transferred through 1.0-km (Fig. 3A) and 3.0-km (Fig. 3B) fibers, respectively. First, the QNLs are measured by blocking all signal modes, which are shown as black curves in Fig. 3. Then, if the EPR entangled state is blocked while other light beams are opened, the corresponding classical teleportation is achieved (4). To realize the teleportation of an unknown state, the classical signals measured by Alice have to be faithfully transmitted to Bob without distortion and with proper phase shift and gain. The measured noise powers of the output state (blue curves in Fig. 3) are 4.8 dB above the corresponding QNLs for both quadrature amplitude and phase, that is, because extra two

units of vacuum noise have been introduced to the system under the present condition (4). The exact teleportation gain is 0.96 ± 0.04 and 0.96 ± 0.05 for amplitude quadrature and phase quadrature, respectively. The method for measuring teleportation gain is given in Materials and Methods. After the EPR entangled state is distributed to Alice and Bob, noise powers of the teleported state measured by Victor are 1.99 ± 0.13 dB and 1.30 ± 0.19 dB below the noise levels of the corresponding classical teleportation, respectively, for transmission distances of 2.0 and 6.0 km, which are shown as red curves in Fig. 3 (A and B). Substituting the measured values into Eq. 2, fidelities (F) of 0.69 ± 0.02 and 0.62 ± 0.03 are obtained, which are in reasonable agreement with the theoretically calculated results with the same system parameters.

The Wigner function, which is known as a quasi-probability distribution of quadrature amplitude and phase in phase space, provides the complete quantum characteristics of a quantum state (36, 37). To intuitively observe the quality of quantum teleportation with different transmission distances, Wigner functions of the initial state and the teleported resultant states are reconstructed in Victor's station, as shown in Fig. 4. The detailed tomography method and the calculation for the density matrix of the teleported state are given in the Supplementary Materials. Figure 4A is the reconstructed Wigner function for the initial input coherent state prepared by Victor. Figure 4B (Figure 4C) is the reconstructed Wigner function for the output state after quantum teleportation with a transmission distance of 2.0 km (6.0 km) between two communicating partners Alice and Bob.

The gain factor g of the classical channels plays an important role in quantum teleportation. If unity gain is selected, then arbitrary quantum state can be transferred with the presented system. Thus, unity gain is chosen in typical experiments (4, 9, 24–27). The influence of teleportation gains on fidelity is analyzed in Fig. 5, where the blue and red curves correspond to transmission distances of 2.0 and 6.0 km, respectively. When the value of g deviates from unity value (0 dB in Fig. 5), fidelity drops quickly. The blue and red squares mark the experimental results, which are in reasonable agreement with the theoretical values.

DISCUSSION

In conclusion, based on the generation of EPR entangled states at a wavelength close to the fiber transmission window, we experimentally
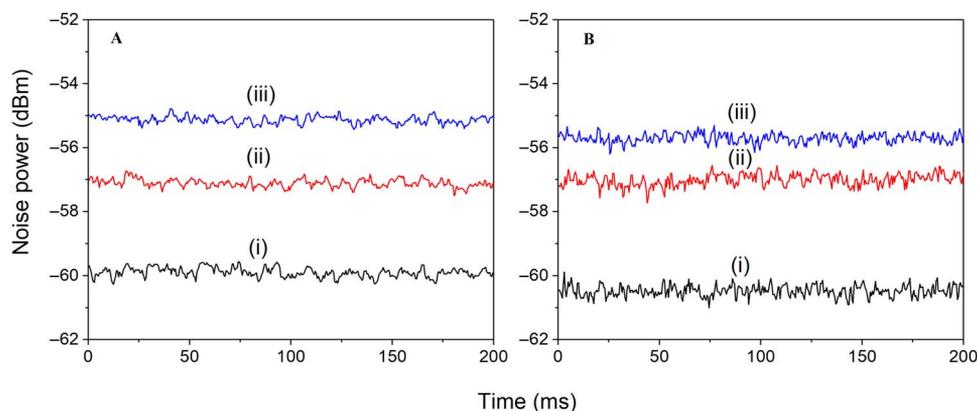

Fig. 3. Noise powers of the teleported state measured by Victor at 3.0 MHz. The measured noise power of the quantum teleported state over transmission distances of 2.0 km (**A**) and 6.0 km (**B**) between Alice and Bob. Curves (i), (ii), and (iii) are the corresponding QNLs of Victor's detection, the noise power of the output state of quantum teleportation with EPR entanglement, and the noise power of teleportation without EPR entanglement (classical teleportation), respectively. The noise power of the quantum teleported output state is 1.99 ± 0.13 dB (1.30 ± 0.19 dB) below that of a classical teleported output state over a transmission distance of 2.0 km (6.0 km).
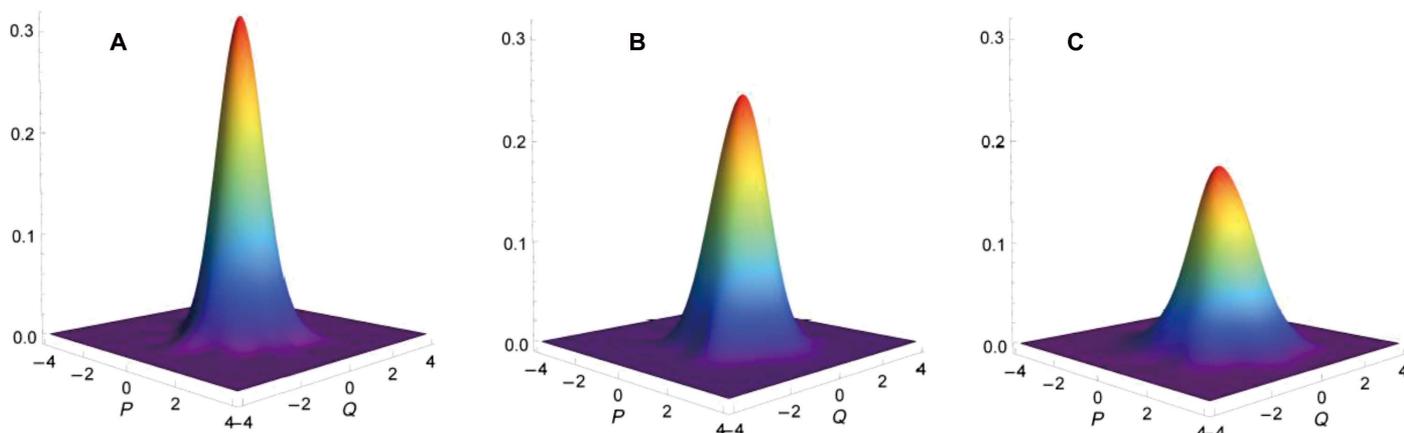
Fig. 4. Reconstructed Wigner functions of input and output states of quantum teleportation through a fiber channel. (**A**) Reconstructed Wigner function of the input coherent state. Reconstructed Wigner function of the quantum teleported state over transmission distances of 2.0 km (**B**) and 6.0 km (**C**).
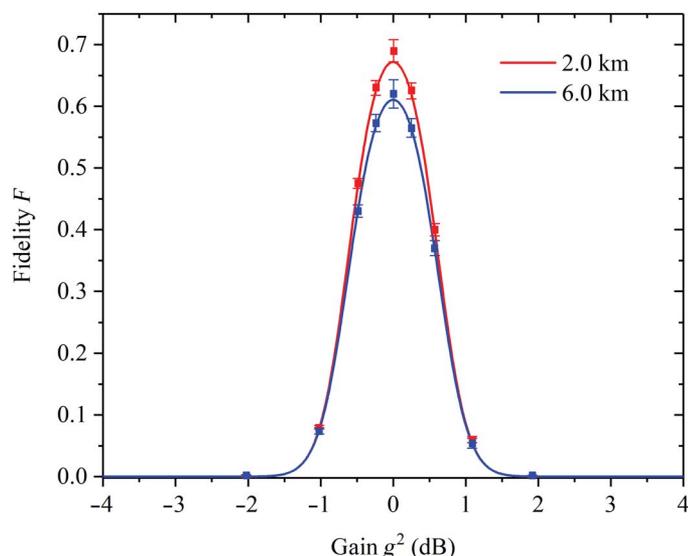

Fig. 5. Fidelity of quantum teleportation versus the teleportation gain g for different communication lengths between Alice and Bob. In our experiment, the teleportation gains of amplitude quadrature and phase quadrature always take the same values ($g_x = g_p = g$) because the two quadrature components are symmetric. The blue and red curves express the dependences of calculated fidelities on the teleportation gain (g) when the transmission distance is 2.0 and 6.0 km, respectively. When $g = 1$ (0 dB) is selected in the experiment, the best fidelity can be obtained for both conditions. The squares mark the experimental results, which are in reasonable agreement with the theoretical values. Error bars represent the SE and are obtained from the statistics of the fidelity.

demonstrated deterministic CV quantum teleportation of a coherent state at a distance of several kilometers. The fidelities we achieved are 0.62 ± 0.03 and 0.69 ± 0.02 for 6.0- and 2.0-km communication distances, which are higher than the classical teleportation limit and the no-cloning limit, respectively (29). The fidelity depends on the quantum correlations of the EPR entangled state distributed to a sending station (Alice) and a receiving station (Bob). Although the correlation degree of the initial EPR entangled state is about 5.2 dB in both amplitude quadrature and phase quadrature, it is reduced to only 2.2 dB when the sub-mode of the EPR entangled state is transmitted through a

3.0-km fiber due to the existence of transmission losses and GAWBS extra noise. The calculated fidelity between the input state and the output state according to the experimental values is only 0.62. In the current experiment, the power of EPR entanglement and the corresponding LO beam are respectively controlled to several microwatts and several hundred microwatts to reduce the influence of GAWBS extra noise. When longer fibers are used, larger optical losses and GAWBS extra noise will be introduced into the experimental system inevitably, which might result in further destruction of quantum correlations of the EPR entangled state. If EPR entanglement is enhanced, then the distance of quantum teleportation and the fidelity of resultant state will be improved. Although one can reduce the influence of GAWBS noise by only transferring the EPR sub-modes through optical fibers and generating the LO beam at the terminal stations (38), the relative phase between them has to be carefully controlled, and the misadjustment of the relative phase will result in extra noises as well. Another method to reduce the influence of GAWBS noise is to use time- and polarization-multiplexing techniques in the transmission of the input state and the corresponding LO beam (39), in which the continual signal beam and the corresponding LO beam are respectively chopped into a series of optical pulses. By choosing proper pulse duration time and delay time between the two pulses, the signal beam and the LO beam will pass through the fiber at different times, and thus, the influence of GAWBS noise can be greatly restrained. By means of the abovementioned technologies, it is possible to notably extend the distance of quantum teleportation (13, 40).

Quantum teleportation is a basic operation in quantum information science, with which quantum information involved in quantum states can be disembodiedly transmitted, which is impossible by means of any classical communication methods. Besides its theoretical worth in quantum information, it is also a fundamental protocol in quantum technologies. For CV quantum information, if a practical quantum network at the metropolitan scale is designed and built, then quantum teleportation through a several-kilometer channel has to be required. On the basis of the specific advantages of CV quantum teleportation with optical modes, such as high rates and bandwidths, it is necessary to explore the feasible protocol of CV quantum teleportation via optical fiber channels (7–9). Although our current experiment is only realized in the laboratory, it provides a method to realize deterministic quantum teleportation in a several-kilometer

range with fiber channels. Transfer distance can be further improved (i.e., longer distances) by decreasing the influence of GAWBS and enhancing EPR entanglement.

MATERIALS AND METHODS
Experimental setup
The experimental setup is shown in detail in fig. S1. The laser source Nd:YVO$_4$/LBO (Yuguang Co., DPSS FG-VIIIB) was operated with a dual wavelength of 1342 and 671 nm, and the corresponding output powers were about 1.0 and 2.7 W, respectively. The two beams with different wavelengths were separated by a dichroic beam splitter; each beam was then passed through a mode-cleaner-infrared (MCI) and mode-cleaner-red (MCR) to reduce noises in quadrature amplitude and phase and to optimize the spatial modes of beams. In our experiment, the noise of the infrared laser filtered by the MCI reached the QNL at analysis frequencies higher than 2.8 MHz; thus, it can be treated as a coherent state at a frequency of 3.0 MHz. A Fabry-Perot cavity was used to monitor the single-frequency operation of the laser. DOPA1 and DOPA2 were in the same configuration to obtain two analogous squeezed states of light, which will be coupled to produce an EPR entangled state via the interference of spatial modes. The DOPAs had the configuration of a standing-wave optical cavity, which contained a pair of concave mirrors and a type 0 quasi–phase-matched periodically poled KTiOPO$_4$ (PPKTP) crystal with dimensions of 1 mm by 2 mm by 12 mm. The diameters of both concave mirrors are 10 mm, and the curvature radii are 50 mm. The input mirror was coated with film with reflectivity $R > 99.8\%$ at 1342 nm and transmission $T = 20\%$ at 671 nm, and the output mirror was coated with transmission $T = 10\%$ at 1342 nm and reflectivity $R > 99.9\%$ at 671 nm. When both DOPAs work under deamplification conditions, i.e., the relative phase between the pump beam and the seeded signal beam was maintained at $\pi + 2k\pi$ (k is an integer), two quadrature amplitude squeezed states of light with 5.28 ± 0.16 dB and 5.31 ± 0.19 dB below corresponding QNLs were generated by DOPA1 and DOPA2, respectively. Then, the EPR entangled state was obtained by interfering the two squeezed states of light on a 50/50 BS with the relative phase of $\pi/2 + k\pi$ (k is an integer).

The method for measuring teleportation gain
To reduce the influence of GAWBS noise and to maintain the phase locking of balanced homodyne detection, an LO beam power of 0.25 mW was first used. The QNLs [traces (i) in Fig. 3] can be easily obtained by blocking all the optical signals with the exception of the LO beam of Victor's detection. A crucial part of quantum teleportation is the transmission of classical information from Alice to Bob. The classical information is the photocurrents measured by Alice's two homodyne detectors, which have to be faithfully transferred to EPR2 at Bob; thus, the AM and PM used by Bob should be without distortion and with proper phase and gain (4, 31). Half-wave plates before AM and PM must be precisely rotated to ensure that the amplitude modulation and the phase modulation do not disturb each other. According to Eqs. 4 and 5, if the EPR entangled state is not applied in quantum teleportation, the calculated variance should be 3.0 for the teleportation of unity gain; i.e., the variances of both amplitude and phase quadratures should be 4.8 dB higher than the QNL. By carefully adjusting the electric gain of classical information from Alice to Bob, the variances are regulated to 4.8 dB higher than the QNLs [traces (iii) in Fig. 3] and the teleportation gain g is selected as unity value. Last, when the EPR entangled state is used, quantum

teleportation is realized, and the measured variances are shown as traces (ii) in Fig. 3. For other values of teleportation gain, the variances in classical teleportation can be calculated with Eqs. 4 and 5. In the same way, by adjusting the electric gain of classical information, the variances can be regulated to the needed values.

SUPPLEMENTARY MATERIALS
The method to reconstruct the Wigner function of the teleported state
Fig. S1. Experimental setup for fiber-channel CV quantum teleportation.

REFERENCES AND NOTES
1. C. H. Bennett, G. Brassard, C. Crépeau, R. Jozsa, A. Peres, W. K. Wootters, Teleporting an unknown quantum state via dual classical and Einstein-Podolsky-Rosen channels. *Phys. Rev. Lett.* **70**, 1895–1899 (1993).
2. L. Vaidman, Teleportation of quantum states. *Phys. Rev. A* **49**, 1473–1476 (1994).
3. S. L. Braunstein, H. J. Kimble, Teleportation of continuous quantum variables. *Phys. Rev. Lett.* **80**, 869–872 (1998).
4. A. Furusawa, J. L. Sørensen, S. L. Braunstein, C. A. Fuchs, H. J. Kimble, E. S. Polzik, Unconditional quantum teleportation. *Science* **282**, 706–709 (1998).
5. D. Bouwmeester, J.-W. Pan, K. Mattle, M. Eibl, H. Weinfurter, A. Zeilinger, Experimental quantum teleportation. *Nature* **390**, 575–579 (1997).
6. D. Boschi, S. Branca, F. De Martini, L. Hardy, S. Popescu, Experimental realization of teleporting an unknown pure quantum state via dual classical and Einstein-Podolsky-Rosen channels. *Phys. Rev. Lett.* **80**, 1121–1125 (1998).
7. J.-W. Pan, Z.-B. Chen, C.-Y. Lu, H. Weinfurter, A. Žeilinger, M. Zukowski, Multiphoton entanglement and interferometry. *Rev. Mod. Phys.* **84**, 777–838 (2012).
8. X.-X. Xia, Q.-C. Sun, Q. Zhang, J.-W. Pan, Long distance quantum teleportation. *Quantum Sci. Technol.* **3**, 014012 (2018).
9. S. Pirandola, J. Eisert, C. Weedbrook, A. Furusawa, S. L. Braunstein, Advances in quantum teleportation. *Nat. Photonics* **9**, 641–652 (2015).
10. X. Su, C. Tian, X. Deng, Q. Li, C. Xie, K. Peng, Quantum entanglement swapping between two multipartite entangled states. *Phys. Rev. Lett.* **117**, 240503 (2016).
11. J.-W. Pan, D. Bouwmeester, H. Weinfurter, A. Zeilinger, Experimental entanglement swapping: Entangling photons that never interacted. *Phys. Rev. Lett.* **80**, 3891–3894 (1998).
12. K. Makino, Y. Hashimoto, J.-i. Yoshikawa, H. Ohdan, T. Toyama, P. van Loock, A. Furusawa, Synchronization of optical photons for quantum information processing. *Sci. Adv.* **2**, e1501772 (2016).
13. H.-J. Briegel, W. Dür, J. I. Cirac, P. Zoller, Quantum repeaters: The role of imperfect local operations in quantum communication. *Phys. Rev. Lett.* **81**, 5932–5935 (1998).
14. J.-S. Xu, M.-H. Yung, X.-Y. Xu, J.-S. Tang, C.-F. Li, G.-C. Guo, Robust bidirectional links for photonic quantum networks. *Sci. Adv.* **2**, e1500672 (2016).
15. D. Gottesman, I. L. Chuang, Demonstrating the viability of universal quantum computation using teleportation and single-qubit operations. *Nature* **402**, 390–393 (1999).
16. R. Raussendorf, H. J. Briegel, A one-way quantum computer. *Phys. Rev. Lett.* **86**, 5188–5191 (2001).
17. F. Bouchard, R. Fickler, R. W. Boyd, E. Karimi, High-dimensional quantum cloning and applications to quantum hacking. *Sci. Adv.* **3**, e1601915 (2017).
18. I. Marcikic, H. de Riedmatten, W. Tittel, H. Zbinden, N. Gisin, Long-distance teleportation of qubits at telecommunication wavelengths. *Nature* **421**, 509–513 (2003).
19. J. Yin, J.-G. Ren, H. Lu, Y. Cao, H.-L. Yong, Y.-P. Wu, C. Liu, S.-K. Liao, F. Zhou, Y. Jiang, X.-D. Cai, P. Xu, G.-S. Pan, J.-J. Jia, Y.-M. Huang, H. Yin, J.-Y. Wang, Y.-A. Chen, C.-Z. Peng, J.-W. Pan, Quantum teleportation and entanglement distribution over 100-kilometre free-space channels. *Nature* **488**, 185–188 (2012).
20. X.-S. Ma, T. Herbst, T. Scheidl, D. Q. Wang, S. Kropatschek, W. Naylor, B. Wittmann, A. Mech, J. Kofler, E. Anisimova, V. Makarov, T. Jennewein, R. Ursin, A. Zeilinger, Quantum teleportation over 143 kilometres using active feed-forward. *Nature* **489**, 269–273 (2012).
21. H. Takwsue, S. D. Dyer, M. J. Stevens, V. Verma, R. P. Mirin, S. W. Nam, Quantum teleportation over 100 km of fiber using highly efficient superconducting nanowire single-photon detectors. *Optica* **2**, 832–835 (2015).
22. Y.-F. Huang, X.-F. Ren, Y.-S. Zhang, L.-M. Duan, G.-C. Guo, Experimental teleportation of a quantum controlled-NOT gate. *Phys. Rev. Lett.* **93**, 240501 (2004).
23. J.-G. Ren, P. Xu, H.-L. Yong, L. Zhang, S.-K. Liao, J. Yin, W.-Y. Liu, W.-Q. Cai, M. Yang, L. Li, K.-X. Yang, X. Han, Y.-Q. Yao, J. Li, H.-Y. Wu, S. Wan, L. Liu, D.-Q. Liu, Y.-W. Kuang,

Z.-P. He, P. Shang, C. Guo, R.-H. Zheng, K. Tian, Z.-C. Zhu, N.-L. Liu, C.-Y. Lu, R. Shu, Y.-A. Chen, C.-Z. Peng, J.-Y. Wang, J.-W. Pan, Ground-to-satellite quantum teleportation. *Nature* **549**, 70–73 (2017).

24. N. Takei, T. Aoki, S. Koike, K. Yoshino, K. Wakui, H. Yonezawa, T. Hiraoka, J. Mizuno, M. Takeoka, M. Ban, A. Furusawa, Experimental demonstration of quantum teleportation of a squeezed state. *Phys. Rev. A* **72**, 042304 (2005).

25. N. Lee, H. Benichi, Y. Takeno, S. Takeda, J. Webb, E. Huntington, A. Furusawa, Teleportation of nonclassical wave packets of light. *Science* **332**, 330–333 (2011).

26. S. Takeda, T. Mizuta, M. Fuwa, P. van Loock, A. Furusawa, Deterministic quantum teleportation of photonic quantum bits by a hybrid technique. *Nature* **500**, 315–318 (2013).

27. D. V. Sychev, A. E. Ulanov, A. A. Pushkina, E. Tiunov, V. Novikov, A. I. Lvovsky, Entanglement and teleportation between polarization and wave-like encodings of an optical qubit. arXiv: 1712.10206 (2017).

28. F. Grosshans, P. Grangier, Quantum cloning and teleportation criteria for continuous quantum variables. *Phys. Rev. A* **64**, 010301 (2001).

29. S. L. Braunstein, C. A. Fuchs, H. J. Kimble, P. van Loock, Quantum versus classical domains for teleportation with continuous variables. *Phys. Rev. A* **64**, 022321 (2001).

30. M. R. Huo, J. L. Qin, Z. H. Yan, X. J. Jia, K. C. Peng, Generation of two types of nonclassical optical states using an optical parametric oscillator with a PPKTP crystal. *Appl. Phys. Lett.* **109**, 221101 (2016).

31. T. C. Zhang, K. W. Goh, C. W. Chou, P. Lodahl, H. J. Kimble, Quantum teleportation of light beams. *Phys. Rev. A* **67**, 033802 (2003).

32. W. P. Bowen, N. Treps, B. C. Buchler, R. Schnabel, T. C. Ralph, H. A. Bachor, T. Symul, P. K. Lam, Experimental investigation of continuous-variable quantum teleportation. *Phys. Rev. A* **67**, 032302 (2003).

33. O. Lopez, A. Amy-Klein, M. Lours, C. Chardonnet, High-resolution microwave frequency dissemination on an 86-km urban optical link. *Appl. Phys. B* **98**, 723–727 (2010).

34. Y. Li, N. Wang, X. Wang, Z. Bai, Influence of guided acoustic wave Brillouin scattering on excess noise in fiber-based continuous variable quantum key distribution. *J. Opt. Soc. Am. B* **31**, 2379–2383 (2014).

35. W. Yang, S. Shi, Y. Wang, W. Ma, Y. Zheng, K. Peng, Detection of stably bright squeezed light with the quantum noise reduction of 12.6 dB by mutually compensating the phase fluctuations. *Opt. Lett.* **42**, 4553–4556 (2017).

36. M. Hillery, R. F. O'Connell, M. O. Scully, E. P. Wigner, Distribution functions in physics: Fundamentals. *Phys. Rep.* **106**, 121–167 (1984).

37. D. T. Smithey, M. Beck, M. G. Raymer, A. Faridani, Measurement of the Wigner distribution and the density matrix of a light mode using optical homodyne tomography: Application to squeezed states and the vacuum. *Phys. Rev. Lett.* **70**, 1244–1247 (1993).

38. D. Huang, P. Huang, D. Lin, C. Wang, G. Zeng, High-speed continuous-variable quantum key distribution without sending a local oscillator. *Opt. Lett.* **40**, 3695–3698 (2015).

39. P. Jouguet, S. Kunz-Jacques, A. Leverrier, P. Grangier, E. Diamanti, Experimental demonstration of long-distance continuous-variable quantum key distribution. *Nat. Photonics* **7**, 378–381 (2013).

40. R. Valivarthi, M. G. Puigibert, Q. Zhou, G. H. Aguilar, V. B. Verma, F. Marsili, M. D. Shaw, S. W. Nam, D. Oblak, W. Tittel, Quantum teleportation across a metropolitan fibre network. *Nat. Photonics* **10**, 676–680 (2016).

Citation: M. Huo, J. Qin, J. Cheng, Z. Yan, Z. Qin, X. Su, X. Jia, C. Xie, K. Peng, Deterministic quantum teleportation through fiber channels. *Sci. Adv.* **4**, eaas9401 (2018).

Deterministic quantum teleportation through fiber channels

Meiru Huo, Jiliang Qin, Jialin Cheng, Zhihui Yan, Zhongzhong Qin, Xiaolong Su, Xiaojun Jia, Changde Xie and Kunchi Peng

ARTICLE TOOLS	http://advances.sciencemag.org/content/4/10/eaas9401
SUPPLEMENTARY MATERIALS	http://advances.sciencemag.org/content/suppl/2018/10/15/4.10.eaas9401.DC1
REFERENCES	This article cites 39 articles, 5 of which you can access for free http://advances.sciencemag.org/content/4/10/eaas9401#BIBL
PERMISSIONS	http://www.sciencemag.org/help/reprints-and-permissions

Use of this article is subject to the Terms of Service